



Research article

A symbolic computation approach and its application to the Kadomtsev-Petviashvili equation in two (3+1)-dimensional extensions

Weaam Alhejaili¹, Mohammed. K. Elboree^{2,*} and Abdelraheem M. Aly^{3,4}

¹ Department of Mathematical Sciences, College of Science, Princess Nourah bint Abdulrahman University, P.O. Box 84428, Riyadh 11671, Saudi Arabia

² Department of Mathematics, Faculty of Science, South Valley University, Qena 83523, Egypt

³ Department of Mathematics, Faculty of Science, King Khalid University, Abha 62529, Saudi Arabia

⁴ Department of Mathematics, Faculty of Science, South Valley University, Qena 83523, Egypt

* **Correspondence:** Email: mkelboree@gmail.com.

Abstract: This work examines the multi-rogue-wave solutions for the Kadomtsev-Petviashvili (KP) equation in form of two (3+1)-dimensional extensions, which are soliton equations, using a symbolic computation approach. This approach is stated in terms of the special polynomials developed through a Hirota bilinear equation. The first, second, and third-order rogue wave solutions are derived for these equations. The interaction of many rogue waves is illustrated by the multi-rogue waves. The physical explanations and properties of the obtained results are plotted for specific values of the parameters α and β to understand the physics behind the huge (rogue) wave appearance. The figures are represented in three-dimensional, and the contour plots and the density are shown at different values of parameters. The obtained results are significant for showing the dynamic actions of higher-rogue waves in the deep ocean and nonlinear optical fibers.

Keywords: (3+1)-KP equation; bilinear form; symbolic computation approach; rogue waves

Mathematics Subject Classification: 35Q58, 35Q99, 34A34

1. Introduction

The soliton solutions of nonlinear evolution equations (NLEE) play an important role to understand the various advantages of physical phenomena in fluids, plasmas, etc [1, 2]. Rational solutions are a particular type of soliton solutions, which include lump and rogue waves.

A rogue wave which is a type of rational solution is isolated. It is reported in [3, 4] that the mean height of rogue waves is at least double times the height of the neighboring waves. Rogue waves come

from nowhere and disappear with no trace [5, 6] and superfluids [7]. The applications of rogue waves with their rational solutions for the Boussinesq equation can be found in [8].

Rogue waves can be seen in the thick ocean [7, 9], water tanks [10, 11], and optical fibers [10, 12].

The purpose for the rogue wave is to understand the physics of the huge waves appearance and its relations to the environmental conditions (wind and atmospheric pressure).

In the literature, many methods were proposed to derive the rogue wave solutions such as an inverse scattering method [13], Hirota bilinear method [14], Darboux transformation method [15], Bäcklund transformation method [16], variational direct method, simplified extended tanh-function method, Exp-function method, extended rational Sin-Cos and sinh-cosh methods. In [17] the author derives the periodic wave solution for the fractional complex nonlinear Fokas-Lenells equation via an ancient Chinese algorithm so called the Ying Bu Zu Shu. Also in [18] the authors deduced the abundant solitons and periodic solutions of the (1+2)-dimensional chiral nonlinear Schrödinger equation using the extended He's variational method. In [19] the same authors gave the explicit solutions for the Benney-Luke equation in dark solitary, dark-like solitary, kinky dark solitary and periodic wave solutions by the variational direct method (VDM).

The KP equation is a nonlinear partial differential equation in one temporal and two or three spatial coordinate, describes the evolution of nonlinear long waves for small amplitudes.

Furthermore, the (KP) equation was proposed to deal with slowly varying perturbation wave in dispersion media. This equation has been studied in a variety of scientific fields, such as solid state, physics, plasma physics, fiber optics, propagation of waves, oceanography [20].

The importance of the nonlinear terms is to obtain the rogue waves which are nonlinear waves phenomena, so they can be represented with a variety of nonlinear wave equations. Bilinear equation was obtained for soliton equation only and can be used to handle the nonlinear wave equations.

The novelty of this work is handling the higher-order rogue wave solution by the (KP) equation in form of two (3+1)-dimensional extensions

The multi-rogue wave solutions are found for the (3+1)-dimensional Jimbo-Miwa equation [21] and (3+1)-dimensional Hirota bilinear equation based on the bilinear form for this equation using a symbolic computation approach [22]. It is noted that there are similarity between the results in the references [21, 22] and the obtained results in this paper which prove the correctness of the proposed approach.

N-soliton solutions are obtained based on the simplified Hirota approach and kinky-lump breather, combo line kink and kinky-lump breather are derived for (3+1)-dimensional Sharma-Tasso-Olver-like (STOL) model [23]. By the bilinear form for the extended BKPA-Boussinesq equation the abundant breather waves, multi-shocks waves and localized excitation solutions are obtained [24].

The symbolic computation approach method was chosen because it is a simple method to obtain the higher order rogue wave solution without need to obtain a Darboux transformation [25].

Multi rogue waves of the Boussinesq type equation [26–28].

A rogue wave can be formed when wave energy is focused, usually during a storm. When the storm produces waves that go against the prevailing ocean current, the wave frequency shortens.

In [29] the authors constructed the multiple lump solutions of the (3+1)-dimensional potential Yu-Toda-Sasa-Fukuyama equation in fluid dynamics, in [30] the authors studied (2+1)-dimensional asymmetrical Nizhnik-Novikov-Veselov equation. By adding some new constraints to the N-soliton solutions and the resonance Y-type soliton and in [31] the authors investigated the multiple lump

solutions for the generalized (3+1)-dimensional KP equation. With the aid of the variable transformation

In this work, section 2 introduces the description of the symbolic computation approach [32]. Section 3 introduces the multi-rogue waves and bilinear system of the first extended (3+1)-dimensional KP equation. The first, second, and third-order rogue waves for this equation are derived in subsections 3.1–3.3. Section 4 introduces the multi-rogue waves and bilinear form of the second extended (3+1)-dimensional KP equation. Subsections 4.1–4.3 introduces the derivations of the first, second, and third-order rogue waves for this equation. Section 5 introduces the results and conclusions of the outcome results.

2. Materials and methods

The nonlinear partial differential equations (NLEEs) are:

$$H(u, u_t, u_x, u_y, u_z, u_{xt}, u_{xy}, u_{xz} \dots) = 0. \quad (2.1)$$

Here, H is a function in $u(x, y, z, t)$ and its derivatives.

The main steps of the proposed approach are:

Step 1. Following the Painlevé analysis

$$u(x, y, z, t) = u(\zeta, z). \quad (2.2)$$

Step 2. By using (2.2) in NLEEs (2.1), the Hirota's bilinear form is:

$$F(D_\zeta, D_z) = 0, \quad (2.3)$$

where $\zeta = x + y - et$. The D-operator is defined by [33]

$$D_x^k D_y^m D_z^n D_t^l g(x, y, z, t) \cdot f(x, y, z, t) = (-1)^{k+m+n+l} \left(\frac{\partial}{\partial x'} - \frac{\partial}{\partial x} \right)^k \left(\frac{\partial}{\partial y'} - \frac{\partial}{\partial y} \right)^m \left(\frac{\partial}{\partial z'} - \frac{\partial}{\partial z} \right)^n \left(\frac{\partial}{\partial t'} - \frac{\partial}{\partial t} \right)^l [f(x, y, z, t)g(x', y', z', t')] \Big|_{x'=x, y'=y, z'=z, t'=t}. \quad (2.4)$$

Step 3. Let

$$F = G_{n+1}(\zeta, z; \alpha, \beta) = 2\alpha z P_n(\zeta, z) + F_{n+1}(\zeta, z) + 2\beta(\zeta) Q_n(\zeta, z) + (\alpha^2 + \beta^2) F_{n-1}(\zeta, z), \quad (2.5)$$

where

$$\begin{aligned} F_n(\zeta, z; \alpha, \beta) &= \sum_{k=0}^{\frac{1}{2}n(n+1)} \left(\sum_{i=0}^k z^{2i} a_{n(n+1)-2k, 2i} \zeta^{n(n+1)-2k} \right), \\ P_n(\zeta, z) &= \sum_{k=0}^{\frac{1}{2}n(n+1)} \left(\sum_{i=0}^k z^{2i} b_{n(n+1)-2k, 2i} \zeta^{n(n+1)-2k} \right), \\ Q_n(\zeta, z) &= \sum_{k=0}^{\frac{1}{2}n(n+1)} \left(\sum_{i=0}^k z^{2i} c_{n(n+1)-2k, 2i} \zeta^{n(n+1)-2k} \right). \end{aligned} \quad (2.6)$$

$F_0 = 1, F_{-1} = P_0 = Q_0 = 0, \alpha, \beta, a_{m,l}, b_{m,l}$ and $c_{m,l}, (m, l = 0, 2, 4, \dots, n(n+1))$ are real numbers. α, β are used to control the rogue-wave center.

Step 4. By substituting (2.5) into (2.3) and taking the coefficients of z and ζ equal to zero, a system of polynomials is obtained.

Step 5. For getting the multi rogue wave solutions in terms of z and ζ , the values of $a_{m,l}, b_{m,l}$ and $c_{m,l}$ are substituted into (2.5).

3. The bilinear form and multi rogue waves for the first extended (3+1)-dimensional KP equation

The first extended (3+1)-dimensional KP equation [34]:

$$(u_t + \delta u u_x + \mu u_{xxx})_x + \chi(u_{xx} + u_{yy} + u_{zz}) = 0, \quad (3.1)$$

where δ, μ and χ are plasma parameters. And u is a wave amplitude functions in x, y, z and t . The rogue-waves solutions for (3.1) can be obtained by finding the Hirota bilinear form.

In (3.1) setting $\zeta = x + dy - et$,

$$\mu u_{\zeta\zeta\zeta\zeta} + (d^2\chi + \delta u - e + \chi)u_{\zeta\zeta} + \delta u_{\zeta}^2 + \chi u_{zz} = 0. \quad (3.2)$$

Using the following variable transformation

$$u = u_0 + \frac{12\mu}{\delta}(\ln F)_{\zeta\zeta}. \quad (3.3)$$

Where u_0 is a constant, the Hirota bilinear form for (3.1) is obtained by substituting (3.3) into (3.2):

$$(\mu D_{\zeta}^4 + (d^2\chi + \delta u_0 - e + \chi)D_{\zeta}^2 + \chi D_z^2)F \cdot F = 0. \quad (3.4)$$

If $\chi = 1, \mu = -(1/3), e = d^2 + \delta u_0$, then (3.1) converts to the Boussinesq equation [8].

The multi rogue wave solutions of the first extended (3+1)-dimensional (KP) equation (3.1) can be obtained as follows.

3.1. First-order rogue waves $n = 0$

Here, F is selected as

$$F = G_1 = a_{2,0}\zeta^2 + a_{0,2}z^2 + a_{0,0}. \quad (3.5)$$

Let $a_{2,0} = 1$ with no loss of generalization.

The coefficients $a_{0,0}$ and $a_{0,2}$ are obtained by substituting (3.5) into (3.4) and taken zero value for the coefficients of all powers of z and ζ

$$a_{0,0} = -\frac{3\mu}{d^2\chi + \delta u_0 + \chi - e}, \quad a_{0,2} = \frac{d^2\chi + \delta u_0 + \chi - e}{\chi}. \quad (3.6)$$

The first-order rogue waves of Eq (3.1) is obtained by inserting (3.6) in (3.5) we get

$$u = u_0 + \frac{12\mu}{\delta}(\ln G_1)_{\zeta\zeta}, \quad (3.7)$$

where

$$G_1 = \frac{(d^2\chi + \delta u_0 + \chi - e)(z - \alpha)^2}{\chi} + (\zeta - \beta)^2 - \frac{3\mu}{d^2\chi + \delta u_0 + \chi - e}. \tag{3.8}$$

Figure 1 shows first-order rogue wave solutions (3.7) at $\alpha = \beta = 0$. These solutions have three centers $(0, 0)$ and $(\pm 3 \sqrt{-\frac{\mu}{d^2\chi + \delta u_0 + \chi - e}}, 0)$. In three-dimensional, contour plot and the corresponding density plot is presented. It is remarked that there is one peak, and the first-order rogue wave has the minimum amplitude $-\frac{8d^2\chi + 7\delta u_0 + 8\chi - 8e}{\delta}$ at $(0, 0)$ and maximal amplitude $\frac{d^2\chi + 2\delta u_0 + \chi - e}{\delta}$ at $(3 \sqrt{-\frac{\mu}{d^2\chi + \delta u_0 + \chi - e}}, 0)$ when $\mu > 0, d^2\chi + \delta u_0 + \chi < e$. The first-order rogue wave solutions (3.7) at $\alpha = -5, \beta = -5$ the center of rogue wave will be $(-5, -5)$ and $(\frac{-5d^2\chi - 5\delta u_0 + 3\sqrt{-\chi d^2\mu - \delta\mu u_0 - \chi\mu + \delta\mu e - 5\chi + 5e}}{d^2\chi + \delta u_0 + \chi - e}, -5)$ as shown in Figure 2, moreover, the minimal and maximal amplitudes also change into $-\frac{8d^2\chi + 7\delta u_0 + 8\chi - 8e}{\delta}$ and $\frac{d^2\chi + 2\delta u_0 + \chi - e}{\delta}$ respectively.

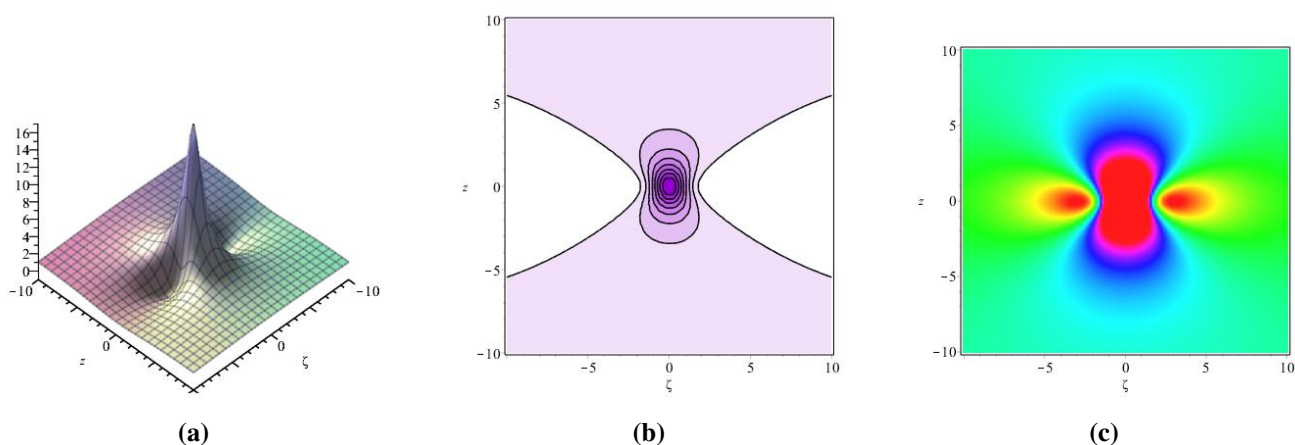


Figure 1. The first-order rogue wave solution (3.7). (a) 3D plot; (b) Contour plot; (c) Density at $\alpha = \beta = 0$.

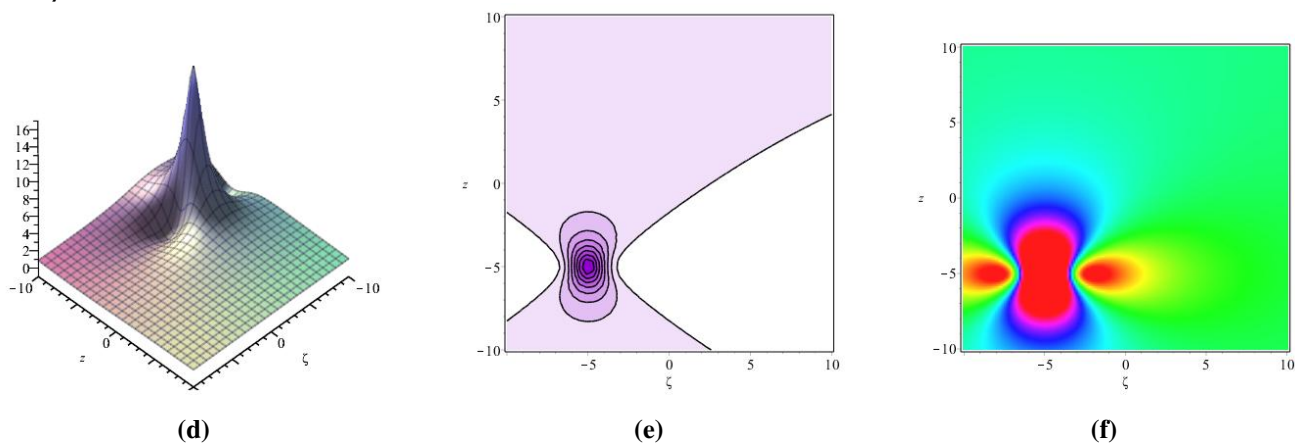


Figure 2. The first-order rogue wave solution (3.7). (d) 3D plot; (e) Contour plot; (f) Density at $\alpha = \beta = -2$.

3.2. Second-order rogue waves $n = 1$

The second-order rogue wave solutions of Eq (3.1) can be found by setting $n = 1$ in Eq (2.5) as:

$$F = G_2(\zeta, z; \alpha, \beta) = 2\alpha z P_1(\zeta, z) + F_2(\zeta, z) + 2\beta \zeta Q_1(\zeta, z) + (\alpha^2 + \beta^2) F_0(\zeta, z) = \\ a_{6,0} \zeta^6 + (z^2 a_{4,2} + a_{4,0}) \zeta^4 + 2\zeta^3 \beta c_{2,0} + (z^4 a_{2,4} + 2\alpha z b_{2,0} + z^2 a_{2,2} + a_{2,0}) \zeta^2 + 2\beta \\ (c_{0,2} z^2 + c_{0,0}) \zeta + a_{0,6} z^6 + a_{0,4} z^4 + 2\alpha z^3 b_{0,2} + a_{0,2} z^2 + 2\alpha z b_{0,0} + a_{0,0} (\alpha^2 + \beta^2 + 1). \quad (3.9)$$

Substituting (3.9) in (3.4) and taking the coefficients of all powers of ζ and z equal to zero, the set of parameters $a_{m,l}, b_{m,l}, c_{m,l}, (m, l = 0, 2, 4, 6)$ can be obtained as:

$$a_{0,0} = \frac{1}{9((d^2 + 1)\chi + \delta u_0 - e)^3(\alpha^2 + \beta^2 + 1)} (9(c_{2,0}^2(d^2 + 1)\beta^2 + \frac{1}{9}\alpha^2 b_{2,0}^2)(d^2 + 1)^2 \chi^3 \\ - 27(c_{2,0}^2(d^2 + 1)\beta^2 + \frac{2\alpha^2 b_{2,0}^2}{27})(d^2 + 1)(-\delta u_0 + e)\chi^2 + 27(c_{2,0}^2(d^2 + 1)\beta^2 + \frac{1}{27}\alpha^2 b_{2,0}^2) \\ \times (-\delta u_0 + e)^2 \chi - 9c_{2,0}^2(-\delta u_0 + e)^3 \beta^2 - 16875\mu^3), a_{0,2} = \frac{475\mu^2}{\chi(d^2\chi + \delta u_0 + \chi - e)}, \\ a_{0,4} = -\frac{17\mu(d^2\chi + \delta u_0 + \chi - e)}{\chi^2}, a_{0,6} = \frac{(d^2\chi + \delta u_0 + \chi - e)^3}{\chi^3}, \\ a_{2,0} = -\frac{125\mu^2}{(d^2\chi + \delta u_0 + \chi - e)^2}, a_{2,2} = -\frac{90\mu}{\chi}, a_{2,4} = \frac{3(d^2\chi + \delta u_0 + \chi - e)^2}{\chi^2}, \\ a_{4,0} = -\frac{25\mu}{d^2\chi + \delta u_0 + \chi - e}, a_{4,2} = \frac{3d^2\chi + 3\delta u_0 + 3\chi - 3e}{\chi}, \\ b_{0,0} = -\frac{5\mu b_{2,0}}{3d^2\chi + 3\delta u_0 + 3\chi - 3e}, b_{0,2} = -\frac{b_{2,0}(d^2\chi + \delta u_0 + \chi - e)}{3\chi}, \\ c_{0,0} = \frac{\mu c_{2,0}}{d^2\chi + \delta u_0 + \chi - e}, c_{0,2} = -3\frac{(d^2\chi + \delta u_0 + \chi - e)c_{2,0}}{\chi}, \quad (3.10)$$

where $b_{2,0}$ and $c_{2,0}$ are arbitrary parameters.

The second-order rogue wave of Eq (3.1) can be found as:

$$u = u_0 + \frac{12\mu}{\delta} (\ln G_2(\zeta, z; \alpha, \beta))_{\zeta\zeta}. \quad (3.11)$$

Figures 3 and 4 show the two high peaks of the second-order rogue waves for (3.11) at $\alpha = \beta = 0$. The second-order peak breaks apart and for sufficiently big parameters at $\alpha = \beta = 1000$. The set of three first order rogue waves are forming a triangle called rogue wave triplet.

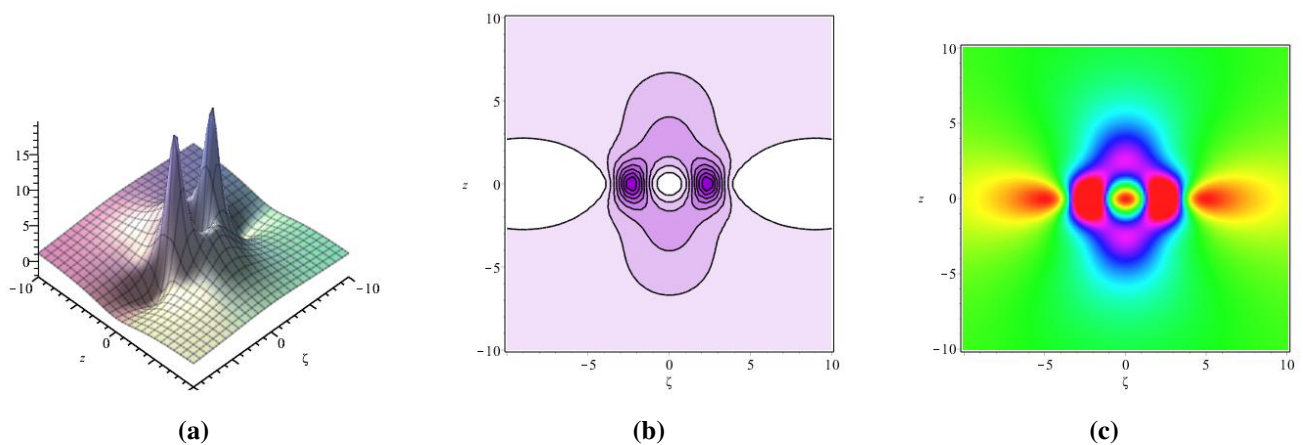


Figure 3. The second-order rogue wave solution (3.11). (a) 3D plot; (b) Contour plot; (c) Density at $\alpha = \beta = 0$.

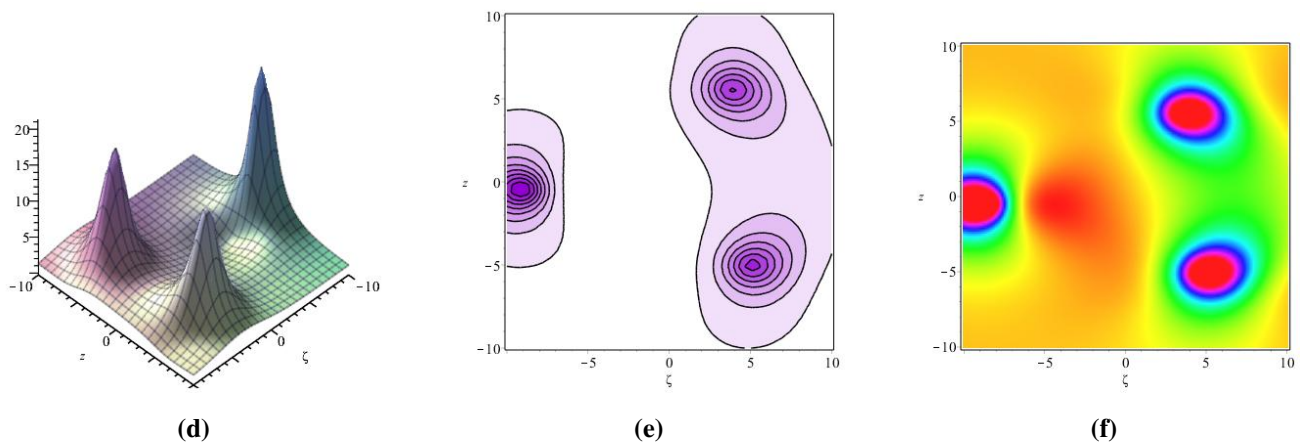


Figure 4. The second-order rogue wave solution (3.11). (d) 3D plot; (e) Contour plot; (f) Density at $\alpha = \beta = 1000$.

3.3. Third-order rogue waves $n = 2$

The third-order rogue wave of Eq (3.1) is given by establishing $n = 2$ in Eq (2.5) as follows:

$$\begin{aligned}
 F &= G_3(\zeta, z; \alpha, \beta) = 2\alpha z P_2(\zeta, z) + F_3(\zeta, z) + 2\beta \zeta Q_2(\zeta, z) + (\alpha^2 + \beta^2) F_1(\zeta, z) \\
 &= a_{12,0} \zeta^{12} + a_{10,0} \zeta^{10} + a_{10,2} z^2 \zeta^{10} + a_{8,0} \zeta^8 + a_{8,2} z^2 \zeta^8 + a_{8,4} z^4 \zeta^8 + \zeta^6 + a_{6,2} z^2 \zeta^6 + a_{6,4} z^4 \zeta^6 \\
 &\quad + a_{6,6} z^6 \zeta^6 + a_{4,0} \zeta^4 + a_{4,2} z^2 \zeta^4 + a_{4,4} z^4 \zeta^4 + a_{4,6} z^6 \zeta^4 + a_{4,8} z^8 \zeta^4 + a_{2,0} \zeta^2 + a_{2,2} z^2 \zeta^2 \\
 &\quad + a_{2,4} z^4 \zeta^2 + a_{2,6} z^6 \zeta^2 + a_{2,8} z^8 \zeta^2 + a_{2,10} z^{10} \zeta^2 + 2\beta (c_{6,0} \zeta^6 + c_{4,2} z^2 \zeta^4 + c_{4,0} \zeta^4 + c_{2,4} z^4 \zeta^2 \\
 &\quad + c_{2,2} z^2 \zeta^2 + c_{2,0} \zeta^2 + c_{0,6} z^6 + c_{0,4} z^4 + c_{0,2} z^2 + c_{0,0}) (\zeta) + (\alpha^2 + \beta^2) (a_{2,0} \zeta^2 + a_{0,2} z^2 \\
 &\quad + a_{0,0}) + a_{0,0} + 2\alpha z (b_{6,0} \zeta^6 + b_{4,2} z^2 \zeta^4 + b_{4,0} \zeta^4 + b_{2,4} z^4 \zeta^2 + b_{2,2} z^2 \zeta^2 + b_{2,0} \zeta^2 + b_{0,6} z^6 \\
 &\quad + b_{0,4} z^4 + b_{0,2} z^2 + b_{0,0}) + a_{0,2} z^2 + a_{0,4} z^4 + a_{0,6} z^6 + a_{0,8} z^8 + a_{0,10} z^{10} + a_{0,12} z^{12}. \quad (3.12)
 \end{aligned}$$

Substituting (3.12) in (3.4) and taken all coefficients of all powers of ζ and z equal to zero, the set of parameters $a_{m,l}, b_{m,l}, c_{m,l}, (m, l = 0, 2, 4, 6)$ are found as:

$$\begin{aligned}
 a_{0,0} &= \frac{1}{1863225 ((d^2 + 1)\chi + \delta u_0 - e)^6 \mu (\alpha^2 + \beta^2 + 1)} (-33075 (d^2 + 1)^6 \\
 &\times (\beta^2 d^2 c_{4,0}^2 + \beta^2 c_{4,0}^2 + \frac{169 \alpha^2 b_{4,0}^2}{11025}) \chi^7 + 231525 (-\delta u_0 + e) (d^2 + 1)^5 (\beta^2 d^2 c_{4,0}^2 + \beta^2 c_{4,0}^2 \\
 &+ \frac{338 \alpha^2 b_{4,0}^2}{25725}) \chi^6 - 694575 (-\delta u_0 + e)^2 (\beta^2 d^2 c_{4,0}^2 + \beta^2 c_{4,0}^2 + \frac{169 \alpha^2 b_{4,0}^2}{15435}) (d^2 + 1)^4 \chi^5 \\
 &+ 1157625 (\beta^2 d^2 c_{4,0}^2 + \beta^2 c_{4,0}^2 + \frac{676 \alpha^2 b_{4,0}^2}{77175}) (-\delta u_0 + e)^3 (d^2 + 1)^3 \chi^4 - 1157625 (-\delta u_0 \\
 &+ e)^4 (d^2 + 1)^2 (\beta^2 d^2 c_{4,0}^2 + \beta^2 c_{4,0}^2 + \frac{169 \alpha^2 b_{4,0}^2}{25725}) \chi^3 + 694575 (-\delta u_0 + e)^5 (d^2 + 1) (\beta^2 d^2 c_{4,0}^2 \\
 &+ \beta^2 c_{4,0}^2 + \frac{338 \alpha^2 b_{4,0}^2}{77175}) \chi^2 - 231525 (-\delta u_0 + e)^6 (\beta^2 d^2 c_{4,0}^2 + \beta^2 c_{4,0}^2 + \frac{169 \alpha^2 b_{4,0}^2}{77175}) \chi \\
 &- 33075 \beta^2 \delta^7 u_0^7 c_{4,0}^2 + 231525 \beta^2 \delta^6 e u_0^6 c_{4,0}^2 - 694575 \beta^2 \delta^5 e^2 u_0^5 c_{4,0}^2 + 1157625 \beta^2 \delta^4 e^3 u_0^4 c_{4,0}^2 \\
 &- 1157625 \beta^2 \delta^3 e^4 u_0^3 c_{4,0}^2 + 694575 \beta^2 \delta^2 e^5 u_0^2 c_{4,0}^2 - 231525 \beta^2 \delta e^6 u_0 c_{4,0}^2 + 33075 \beta^2 e^7 c_{4,0}^2 \\
 &+ 181938957825625 \mu^7), \\
 a_{0,2} &= \frac{1}{1863225 ((d^2 + 1)\chi + \delta u_0 - e)^4 \mu^2 \chi (\alpha^2 + \beta^2 + 1)} \\
 &\times (11025 (d^2 + 1)^6 (\beta^2 d^2 c_{4,0}^2 + \beta^2 c_{4,0}^2 + \frac{169 \alpha^2 b_{4,0}^2}{11025}) \chi^7 - 77175 (-\delta u_0 + e) (d^2 + 1)^5 \\
 &\times (\beta^2 d^2 c_{4,0}^2 + \beta^2 c_{4,0}^2 + \frac{338 \alpha^2 b_{4,0}^2}{25725}) \chi^6 + 231525 (-\delta u_0 + e)^2 (\beta^2 d^2 c_{4,0}^2 + \beta^2 c_{4,0}^2 \\
 &+ \frac{169 \alpha^2 b_{4,0}^2}{15435}) (d^2 + 1)^4 \chi^5 - 385875 (\beta^2 d^2 c_{4,0}^2 + \beta^2 c_{4,0}^2 + \frac{676 \alpha^2 b_{4,0}^2}{77175}) (-\delta u_0 + e)^3 (d^2 + 1)^3 \chi^4 \\
 &+ 385875 (-\delta u_0 + e)^4 (d^2 + 1)^2 (\beta^2 d^2 c_{4,0}^2 + \beta^2 c_{4,0}^2 + \frac{169 \alpha^2 b_{4,0}^2}{25725}) \chi^3 \\
 &- 231525 (-\delta u_0 + e)^5 (d^2 + 1) (\beta^2 d^2 c_{4,0}^2 + \beta^2 c_{4,0}^2 + \frac{338 \alpha^2 b_{4,0}^2}{77175}) \chi^2 \\
 &+ 77175 (-\delta u_0 + e)^6 (\beta^2 d^2 c_{4,0}^2 + \beta^2 c_{4,0}^2 + \frac{169 \alpha^2 b_{4,0}^2}{77175}) \chi + 11025 \beta^2 \delta^7 u_0^7 c_{4,0}^2 \\
 &- 77175 \beta^2 \delta^6 e u_0^6 c_{4,0}^2 + 231525 \beta^2 \delta^5 e^2 u_0^5 c_{4,0}^2 - 385875 \beta^2 \delta^4 e^3 u_0^4 c_{4,0}^2 + 385875 \beta^2 \delta^3 e^4 u_0^3 c_{4,0}^2 \\
 &- 231525 \beta^2 \delta^2 e^5 u_0^2 c_{4,0}^2 + 77175 \beta^2 \delta e^6 u_0 c_{4,0}^2 - 11025 \beta^2 e^7 c_{4,0}^2 - 186879449006250 \mu^7), \\
 a_{0,4} &= \frac{16391725 \mu^4}{3 (d^2 \chi + \delta u_0 + \chi - e)^2 \chi^2}, a_{0,6} = -\frac{798980 \mu^3}{3 \chi^3}, a_{0,8} = 4335 \frac{(d^2 \chi + \delta u_0 + \chi - e)^2 \mu^2}{\chi^4}, \\
 a_{0,10} &= -58 \frac{(d^2 \chi + \delta u_0 + \chi - e)^4 \mu}{\chi^5}, a_{0,12} = \frac{(d^2 \chi + \delta u_0 + \chi - e)^6}{\chi^6}, \\
 a_{2,0} &= \frac{1}{1863225 ((d^2 + 1)\chi + \delta u_0 - e)^5 \mu^2 (\alpha^2 + \beta^2 + 1)}
 \end{aligned}$$

$$\begin{aligned}
& \times (11025 (d^2 + 1)^6 (\beta^2 d^2 c_{4,0}^2 + \beta^2 c_{4,0}^2 + \frac{169 \alpha^2 b_{4,0}^2}{11025}) \chi^7 - 77175 (-\delta u_0 + e) (d^2 + 1)^5 \\
& \times (\beta^2 d^2 c_{4,0}^2 + \beta^2 c_{4,0}^2 + \frac{338 \alpha^2 b_{4,0}^2}{25725}) \chi^6 + 231525 (-\delta u_0 + e)^2 (\beta^2 d^2 c_{4,0}^2 + \beta^2 c_{4,0}^2 \\
& + \frac{169 \alpha^2 b_{4,0}^2}{15435}) (d^2 + 1)^4 \chi^5 - 385875 (\beta^2 d^2 c_{4,0}^2 + \beta^2 c_{4,0}^2 + \frac{676 \alpha^2 b_{4,0}^2}{77175}) (-\delta u_0 + e)^3 \\
& \times (d^2 + 1)^3 \chi^4 + 385875 (-\delta u_0 + e)^4 (d^2 + 1)^2 (\beta^2 d^2 c_{4,0}^2 + \beta^2 c_{4,0}^2 + \frac{169 \alpha^2 b_{4,0}^2}{25725}) \chi^3 \\
& - 231525 (-\delta u_0 + e)^5 (d^2 + 1) (\beta^2 d^2 c_{4,0}^2 + \beta^2 c_{4,0}^2 + \frac{338 \alpha^2 b_{4,0}^2}{77175}) \chi^2 + 77175 (-\delta u_0 + e)^6 \\
& \times (\beta^2 d^2 c_{4,0}^2 + \beta^2 c_{4,0}^2 + \frac{169 \alpha^2 b_{4,0}^2}{77175}) \chi + 11025 \beta^2 \delta^7 u_0^7 c_{4,0}^2 - 77175 \beta^2 \delta^6 e u_0^6 c_{4,0}^2 \\
& + 231525 \beta^2 \delta^5 e^2 u_0^5 c_{4,0}^2 - 385875 \beta^2 \delta^4 e^3 u_0^4 c_{4,0}^2 + 385875 \beta^2 \delta^3 e^4 u_0^3 c_{4,0}^2 \\
& - 231525 \beta^2 \delta^2 e^5 u_0^2 c_{4,0}^2 + 77175 \beta^2 \delta e^6 u_0 c_{4,0}^2 - 11025 \beta^2 e^7 c_{4,0}^2 - 99239431541250 \mu^7), \\
a_{2,2} &= 565950 \frac{\mu^4}{(d^2 \chi + \delta u_0 + \chi - e)^3 \chi}, a_{2,4} = 14700 \frac{\mu^3}{\chi^2 (d^2 \chi + \delta u_0 + \chi - e)}, \\
a_{2,6} &= 35420 \frac{(d^2 \chi + \delta u_0 + \chi - e) \mu^2}{\chi^3}, a_{2,8} = -570 \frac{(d^2 \chi + \delta u_0 + \chi - e)^3 \mu}{\chi^4}, \\
a_{2,10} &= 6 \frac{(d^2 \chi + \delta u_0 + \chi - e)^5}{\chi^5}, a_{4,0} = -\frac{5187875 \mu^4}{3 (d^2 \chi + \delta u_0 + \chi - e)^4}, \\
a_{4,2} &= -220500 \frac{\mu^3}{(d^2 \chi + \delta u_0 + \chi - e)^2 \chi}, a_{4,4} = 37450 \frac{\mu^2}{\chi^2}, \\
a_{4,6} &= -1460 \frac{(d^2 \chi + \delta u_0 + \chi - e)^2 \mu}{\chi^3}, a_{4,8} = 15 \frac{(d^2 \chi + \delta u_0 + \chi - e)^4}{\chi^4}, \\
a_{6,0} &= -\frac{75460 \mu^3}{3 (d^2 \chi + \delta u_0 + \chi - e)^3}, a_{6,2} = 18620 \frac{\mu^2}{\chi (d^2 \chi + \delta u_0 + \chi - e)}, \\
a_{6,4} &= -1540 \frac{\mu (d^2 \chi + \delta u_0 + \chi - e)}{\chi^2}, a_{6,6} = 20 \frac{(d^2 \chi + \delta u_0 + \chi - e)^3}{\chi^3}, \\
a_{8,0} &= 735 \frac{\mu^2}{(d^2 \chi + \delta u_0 + \chi - e)^2}, a_{8,2} = -690 \frac{\mu}{\chi}, a_{8,4} = 15 \frac{(d^2 \chi + \delta u_0 + \chi - e)^2}{\chi^2}, \\
a_{10,0} &= -98 \frac{\mu}{d^2 \chi + \delta u_0 + \chi - e}, a_{10,2} = \frac{6 d^2 \chi + 6 \delta u_0 + 6 \chi - 6 e}{\chi}, b_{0,0} = \frac{539 b_{4,0} \mu^2}{9 (d^2 \chi + \delta u_0 + \chi - e)^2}, \\
b_{0,2} &= \frac{7 \mu b_{4,0}}{3 \chi}, b_{0,4} = -\frac{(d^2 \chi + \delta u_0 + \chi - e)^2 b_{4,0}}{15 \chi^2}, b_{0,6} = -\frac{(d^2 \chi + \delta u_0 + \chi - e)^4 b_{4,0}}{105 \mu \chi^3}, \\
b_{2,0} &= 19 \frac{\mu b_{4,0}}{3 d^2 \chi + 3 \delta u_0 + 3 \chi - 3 e}, b_{2,2} = -\frac{38 b_{4,0} (d^2 \chi + \delta u_0 + \chi - e)}{21 \chi},
\end{aligned}$$

$$\begin{aligned}
b_{2,4} &= \frac{3 (d^2\chi + \delta u_0 + \chi - e)^3 b_{4,0}}{35 \mu \chi^2}, b_{4,2} = \frac{(d^2\chi + \delta u_0 + \chi - e)^2 b_{4,0}}{21 \chi \mu}, \\
b_{6,0} &= -\frac{b_{4,0} (d^2\chi + \delta u_0 + \chi - e)}{21 \mu}, c_{0,0} = \frac{12005 c_{4,0} \mu^2}{39 (d^2\chi + \delta u_0 + \chi - e)^2}, \\
c_{0,2} &= -\frac{535 \mu c_{4,0}}{13 \chi}, c_{0,4} = \frac{45 (d^2\chi + \delta u_0 + \chi - e)^2 c_{4,0}}{13 \chi^2}, \\
c_{0,6} &= -\frac{5 (d^2\chi + \delta u_0 + \chi - e)^4 c_{4,0}}{13 \mu \chi^3}, c_{2,0} = 245 \frac{\mu c_{4,0}}{13 d^2\chi + 13 \delta u_0 + 13 \chi - 13 e}, \\
c_{2,2} &= -\frac{230 c_{4,0} (d^2\chi + \delta u_0 + \chi - e)}{13 \chi}, c_{2,4} = \frac{5 (d^2\chi + \delta u_0 + \chi - e)^3 c_{4,0}}{13 \mu \chi^2}, \\
c_{4,2} &= \frac{9 (d^2\chi + \delta u_0 + \chi - e)^2 c_{4,0}}{13 \chi \mu}, c_{6,0} = -\frac{c_{4,0} (d^2\chi + \delta u_0 + \chi - e)}{13 \mu},
\end{aligned} \tag{3.13}$$

where $b_{4,0}$ and $c_{4,0}$ are arbitrary constants.

Then the third-order rogue wave solution for Eq (3.1) is defined as:

$$u = u_0 + \frac{12\mu}{\delta} (\ln G_3(\zeta, z; \alpha, \beta))_{\zeta\zeta}. \tag{3.14}$$

Figures 5 and 6 show three high peaks of the third-order rogue waves for (3.14) at $\alpha = \beta = 0$. The third-order peak breaks apart and for sufficiently big parameters at $\alpha = \beta = 10^8$, the third-order rogue waves consist of five first-order rogue waves. These waves are located in the corners of a pentagon and the other sit in the center.

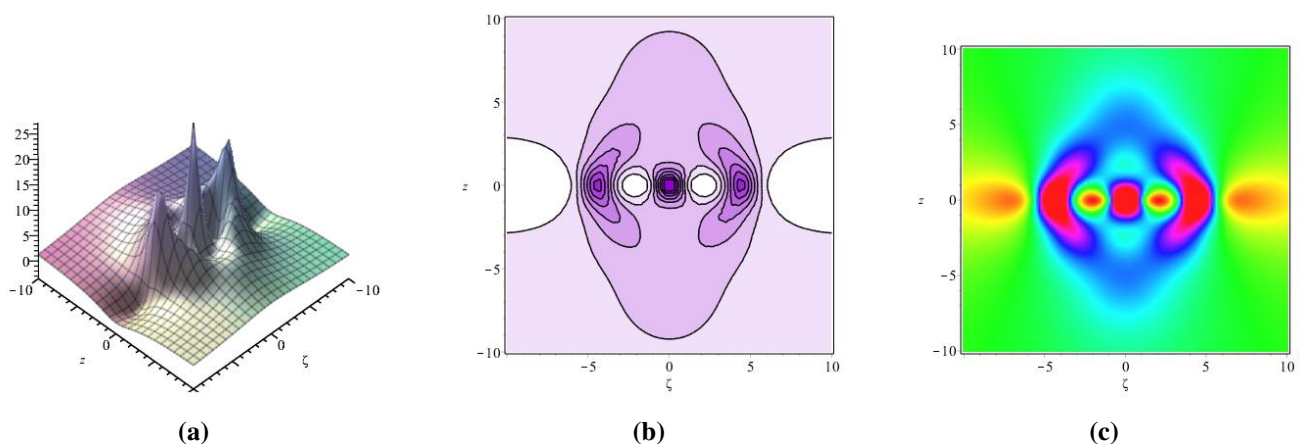


Figure 5. The third-order rogue wave solution (3.14). (a) 3D plot; (b) Contour plot; (c) Density at $\alpha = \beta = 0$.

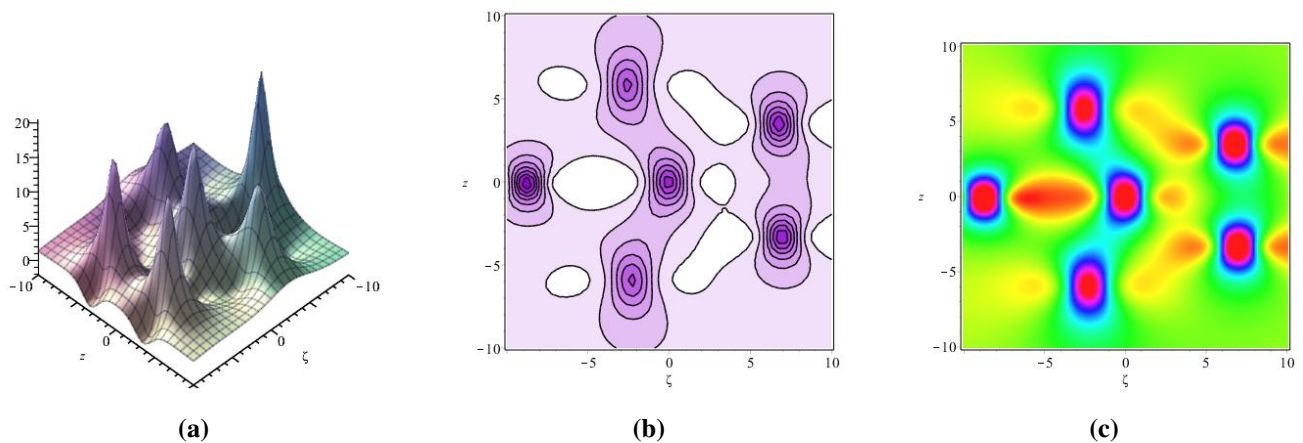


Figure 6. The third-order rogue wave solution (3.14). (d) 3D plot; (e) Contour plot; (f) Density at $\alpha = \beta = 10^8$.

4. The multi rogue waves for the second extended (3+1)-dimensional (KP) equation

The second extended (3+1)-dimensional (KP) equation [34] is:

$$(u_t + \delta uu_x + \mu u_{xxx})_x + \chi(u_{xx} + u_{yy} + u_{zz}) + \rho(u_{xy} + u_{yz} + u_{zx}) = 0, \quad (4.1)$$

where δ, μ, χ and ρ are constants and u is a wave amplitude functions in x, y, z and t .

The rogue-waves solutions for (4.1) can be obtained by finding the Hirota bilinear form by setting $\zeta = x + dy - et$. Then, the ODE of (4.1) can be obtained as:

$$\mu u_{\zeta\zeta\zeta\zeta} + (\delta u - e + 2\chi - \rho)u_{\zeta\zeta} + \delta u_{\zeta}^2 + \chi u_{zz} = 0. \quad (4.2)$$

Using the following variable transformation

$$u = u_0 + \frac{12\mu}{\delta} (\ln F)_{\zeta\zeta}. \quad (4.3)$$

Then we can obtain the Hirota bilinear form for (4.1) by inserting (4.3) into (4.2) as

$$(\mu D_{\zeta}^4 + (\delta u_0 - e + 2\chi - \rho)u_{\zeta\zeta} + \chi D_z^2)F \cdot F = 0. \quad (4.4)$$

The multi rogue wave solutions of the second extended (3+1)-dimensional KP equation (4.1) are given as Figures 7 and 8.

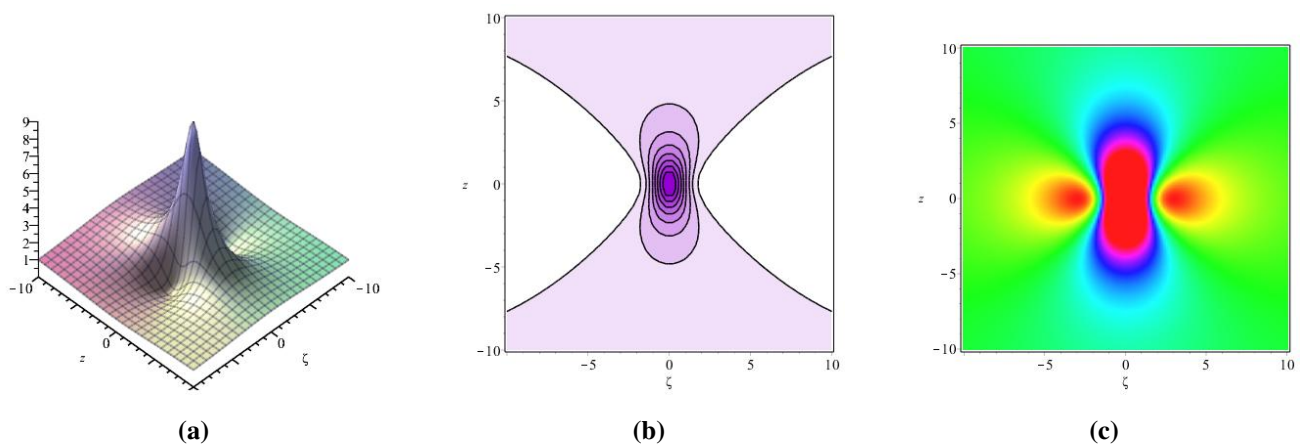


Figure 7. The first-order rogue wave solution (4.6). (a) 3D plot; (b) Contour plot; (c) Density at $\alpha = \beta = 0$.

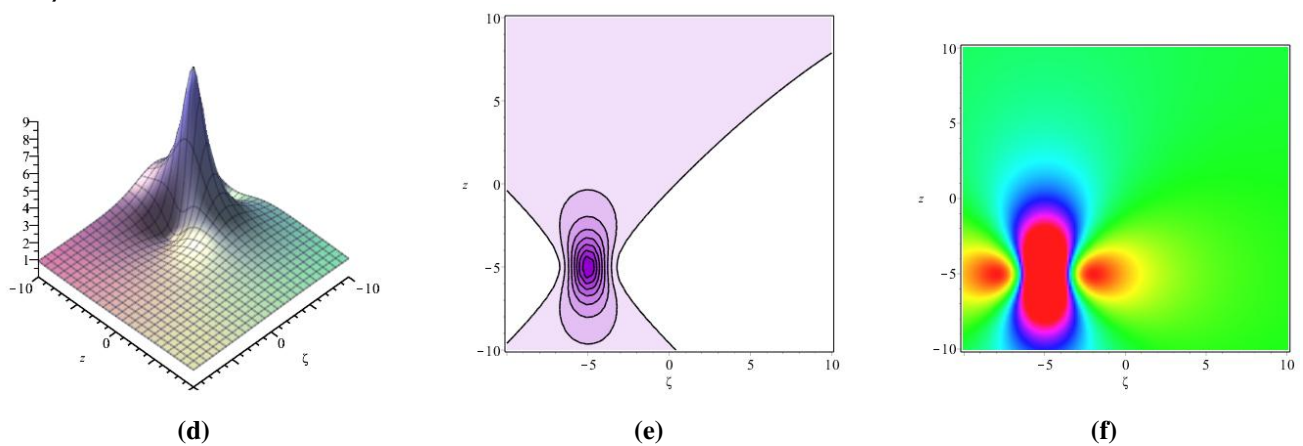


Figure 8. The first-order rogue wave solution (4.6). (d) 3D plot; (e) Contour plot; (f) Density at $\alpha = \beta = -5$.

4.1. Case 1. $n = 0$

The coefficients $a_{0,0}$ and $a_{0,2}$ in Eq (3.5) can be give as follows

$$a_{0,0} = \frac{3\mu}{-\delta u_0 - 2\chi + e + \rho}, \quad a_{0,2} = \frac{\delta u_0 + 2\chi - e - \rho}{\chi}. \quad (4.5)$$

Inserting (4.5) into (3.5), the first-order rogue waves for Eq (4.1) can be obtained in the form

$$u = u_0 + \frac{12\mu}{\delta} (\ln F)_{\zeta\zeta}, \quad (4.6)$$

where

$$F = \frac{\delta u_0 + 2\chi - e - \rho}{\chi} (z - \alpha)^2 + (\zeta - \beta)^2 + \frac{3\mu}{-\delta u_0 - 2\chi + e + \rho}. \quad (4.7)$$

The first-order rogue wave solutions (4.6) when $\alpha = \beta = 0$ are shown in Figure 7. This figure has three centers $(0, 0)$ and $(\pm 3 \sqrt{-\frac{\mu}{\delta u_0 + 2\chi - e - \rho}}, 0)$ in three-dimensional, contour plot and the corresponding

density plot. It is remarked that, there is one peak only because energy of the rogue wave is focused on the high peaks. The first-order rogue wave has the minimal amplitude $\frac{-7\delta u_0 - 16\chi + 8e + 8\rho}{\delta}$ at $(0, 0)$ and maximal amplitude $\frac{2\delta u_0 + 2\chi - e - \rho}{\delta}$ at $(\pm 3\sqrt{-\frac{\mu}{\delta u_0 + 2\chi - e - \rho}}, 0)$ where $\mu > 0, \chi < \frac{1}{2}(-\delta u_0 + e + \rho)$. The first-order rogue wave solutions (4.6) at $\alpha = -5, \beta = -5$ with the centers of rogue wave will be at $(-5, -5)$ and $(\frac{5\delta u_0 - 5e + 10\chi - 5\rho - 3\sqrt{\mu(-\delta u_0 - 2\chi + e + \rho)}}{-\delta u_0 - 2\chi + e + \rho}, -5)$ as shown in Figure 8. The minimal and maximal amplitudes are changing into $\frac{-7\delta u_0 - 16\chi + 8e + 8\rho}{\delta}$ and $\frac{2\delta u_0 + 2\chi - e - \rho}{\delta}$ respectively.

4.2. Case 2. $n = 1$

For this case the second-order rogue wave solutions of Eq (4.1) is:

$$u = u_0 + \frac{12\mu}{\delta} (\ln G_2(\zeta, z; \alpha, \beta))_{\zeta\zeta}, \quad (4.8)$$

where $G_2(\zeta, z; \alpha, \beta)$ is given by (3.9) with $n = 1$ and

$$\begin{aligned} a_{0,0} &= \frac{1}{(9\alpha^2 + 9\beta^2 + 9)(-\delta u_0 - 2\chi + e + \rho)^3} (9c_{2,0}^2(-\delta u_0 - 2\chi + e + \rho)^3\beta^2 - 4\alpha^2\chi^3b_{2,0}^2 \\ &\quad + 4\alpha^2b_{2,0}^2(-\delta u_0 + e + \rho)\chi^2 - \alpha^2b_{2,0}^2(-\delta u_0 + e + \rho)^2\chi + 16875\mu^3), \\ a_{0,2} &= -475\frac{\mu^2}{\chi(-\delta u_0 - 2\chi + e + \rho)}, a_{0,4} = 17\frac{\mu(-\delta u_0 - 2\chi + e + \rho)}{\chi^2}, \\ a_{0,6} &= -\frac{(-\delta u_0 - 2\chi + e + \rho)^3}{\chi^3}, a_{2,0} = -125\frac{\mu^2}{(-\delta u_0 - 2\chi + e + \rho)^2}, a_{2,2} = -90\frac{\mu}{\chi}, \\ a_{2,4} &= 3\frac{(-\delta u_0 - 2\chi + e + \rho)^2}{\chi^2}, a_{4,0} = 25\frac{\mu}{-\delta u_0 - 2\chi + e + \rho}, a_{4,2} = \frac{3\delta u_0 + 6\chi - 3e - 3\rho}{\chi}, \\ b_{0,0} &= -\frac{5\mu b_{2,0}}{3\delta u_0 + 6\chi - 3e - 3\rho}, b_{0,2} = \frac{b_{2,0}(-\delta u_0 - 2\chi + e + \rho)}{3\chi}, c_{0,0} = -\frac{\mu c_{2,0}}{-\delta u_0 - 2\chi + e + \rho}, \\ c_{0,2} &= 3\frac{c_{2,0}(-\delta u_0 - 2\chi + e + \rho)}{\chi}, \end{aligned} \quad (4.9)$$

where $b_{2,0}$ and $c_{2,0}$ is an arbitrary parameters.

In Figures 9 and 10, the two high peaks of the second-order rogue waves of (4.6) at $\alpha = \beta = 0$ are shown. At sufficiently big parameters, the set of three first order rogue waves forms and the centers are formed a triangle entitled a rogue wave triplet.

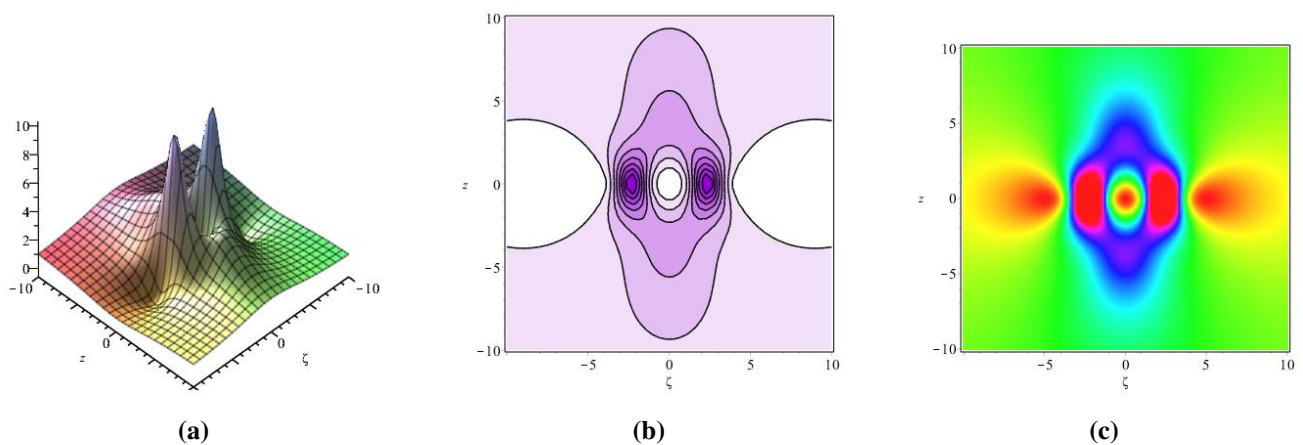


Figure 9. The second-order rogue wave solution (4.8). (a) 3D plot; (b) Contour plot; (c) Density at $\alpha = \beta = 0$.

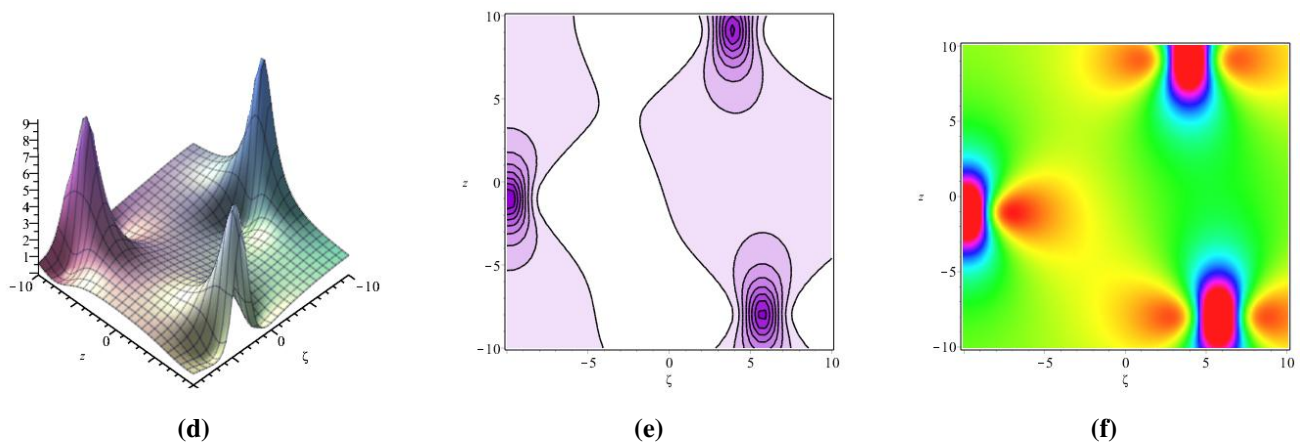


Figure 10. The second-order rogue wave solution (4.8). (a) 3D plot; (b) Contour plot; (c) Density at $\alpha = \beta = 1000$.

4.3. Case 3. $n = 2$

The third-order rogue wave solutions for this case of Eq (4.1) can be obtained as follows

$$u = u_0 + \frac{12\mu}{\delta} (\ln G_3(\zeta, z; \alpha, \beta))_{\zeta\zeta}, \quad (4.10)$$

where $G_3(\zeta, z; \alpha, \beta)$ is given by (3.12) with $n = 2$ and

$$\begin{aligned} a_{0,0} = & \frac{1}{1863225 \mu (\alpha^2 + \beta^2 + 1)(-\delta u_0 - 2\chi + e + \rho)^6} ((-32448 \alpha^2 b_{4,0}^2 - 4233600 c_{4,0}^2 \beta^2) \chi^7 \\ & + 14817600 (c_{4,0}^2 \beta^2 + \frac{169 \alpha^2 b_{4,0}^2}{25725})(-\delta u_0 + e + \rho) \chi^6 - 22226400 (-\delta u_0 + e + \rho)^2 (c_{4,0}^2 \beta^2 \\ & + \frac{169 \alpha^2 b_{4,0}^2}{30870}) \chi^5 + 18522000 (c_{4,0}^2 \beta^2 + \frac{338 \alpha^2 b_{4,0}^2}{77175})(-\delta u_0 + e + \rho)^3 \chi^4 - 9261000 (c_{4,0}^2 \beta^2 \\ & + \frac{169 \alpha^2 b_{4,0}^2}{51450})(-\delta u_0 + e + \rho)^4 \chi^3 + 2778300 (-\delta u_0 + e + \rho)^5 (c_{4,0}^2 \beta^2 + \frac{169 \alpha^2 b_{4,0}^2}{77175}) \chi^2 \end{aligned}$$

$$\begin{aligned}
& -463050(c_{4,0}^2\beta^2 + \frac{169\alpha^2b_{4,0}^2}{154350})(-\delta u_0 + e + \rho)^6\chi - 33075\beta^2\delta^7u_0^7c_{4,0}^2 + 231525c_{4,0}^2\beta^2\delta^6 \\
& \times(e + \rho)u_0^6 - 694575c_{4,0}^2\beta^2\delta^5(e + \rho)^2u_0^5 + 1157625c_{4,0}^2\beta^2\delta^4(e + \rho)^3u_0^4 - 1157625c_{4,0}^2\beta^2\delta^3 \\
& \times(e + \rho)^4u_0^3 + 694575c_{4,0}^2\beta^2\delta^2(e + \rho)^5u_0^2 - 231525c_{4,0}^2\beta^2\delta(e + \rho)^6u_0 + 33075\beta^2e^7c_{4,0}^2 \\
& + 231525\beta^2e^6\rho c_{4,0}^2 + 694575\beta^2e^5\rho^2c_{4,0}^2 + 1157625\beta^2e^4\rho^3c_{4,0}^2 + 1157625\beta^2e^3\rho^4c_{4,0}^2 \\
& + 694575\beta^2e^2\rho^5c_{4,0}^2 + 231525\beta^2e\rho^6c_{4,0}^2 + 33075\beta^2\rho^7c_{4,0}^2 + 181938957825625\mu^7), \\
a_{0,2} = & \frac{1}{(1863225\alpha^2 + 1863225\beta^2 + 1863225)(-\delta u_0 - 2\chi + e + \rho)^4\mu^2\chi}((10816\alpha^2b_{4,0}^2 \\
& + 1411200c_{4,0}^2\beta^2)\chi^7 - 4939200(c_{4,0}^2\beta^2 + \frac{169\alpha^2b_{4,0}^2}{25725})(-\delta u_0 + e + \rho)\chi^6 + 7408800(-\delta u_0 \\
& + e + \rho)^2(c_{4,0}^2\beta^2 + \frac{169\alpha^2b_{4,0}^2}{30870})\chi^5 - 6174000(c_{4,0}^2\beta^2 + \frac{338\alpha^2b_{4,0}^2}{77175})(-\delta u_0 + e + \rho)^3\chi^4 \\
& + 3087000(c_{4,0}^2\beta^2 + \frac{169\alpha^2b_{4,0}^2}{51450})(-\delta u_0 + e + \rho)^4\chi^3 - 926100(-\delta u_0 + e + \rho)^5(c_{4,0}^2\beta^2 \\
& + \frac{169\alpha^2b_{4,0}^2}{77175})\chi^2 + 154350(c_{4,0}^2\beta^2 + \frac{169\alpha^2b_{4,0}^2}{154350})(-\delta u_0 + e + \rho)^6\chi + 11025\beta^2\delta^7u_0^7c_{4,0}^2 \\
& - 77175c_{4,0}^2\beta^2\delta^6(e + \rho)u_0^6 + 231525c_{4,0}^2\beta^2\delta^5(e + \rho)^2u_0^5 - 385875c_{4,0}^2\beta^2\delta^4(e + \rho)^3u_0^4 \\
& + 385875c_{4,0}^2\beta^2\delta^3(e + \rho)^4u_0^3 - 231525c_{4,0}^2\beta^2\delta^2(e + \rho)^5u_0^2 + 77175c_{4,0}^2\beta^2\delta(e + \rho)^6u_0 \\
& - 11025\beta^2e^7c_{4,0}^2 - 77175\beta^2e^6\rho c_{4,0}^2 - 231525\beta^2e^5\rho^2c_{4,0}^2 - 385875\beta^2e^4\rho^3c_{4,0}^2 \\
& - 385875\beta^2e^3\rho^4c_{4,0}^2 - 231525\beta^2e^2\rho^5c_{4,0}^2 - 77175\beta^2e\rho^6c_{4,0}^2 - 11025\beta^2\rho^7c_{4,0}^2 \\
& - 186879449006250\mu^7), a_{0,4} = \frac{16391725\mu^4}{3\chi^2(-\delta u_0 - 2\chi + e + \rho)^2}, \\
a_{0,6} = & -\frac{798980\mu^3}{3\chi^3}, a_{0,8} = 4335\frac{(-\delta u_0 - 2\chi + e + \rho)^2\mu^2}{\chi^4}, \\
a_{0,10} = & -58\frac{\mu(-\delta u_0 - 2\chi + e + \rho)^4}{\chi^5}, a_{0,12} = \frac{(-\delta u_0 - 2\chi + e + \rho)^6}{\chi^6}, \\
a_{2,0} = & \frac{1}{(1863225\alpha^2 + 1863225\beta^2 + 1863225)(-\delta u_0 - 2\chi + e + \rho)^5\mu^2} \\
& \times((-10816\alpha^2b_{4,0}^2 - 1411200c_{4,0}^2\beta^2)\chi^7 + 4939200(c_{4,0}^2\beta^2 + \frac{169\alpha^2b_{4,0}^2}{25725})(-\delta u_0 + e + \rho)\chi^6 \\
& - 7408800(-\delta u_0 + e + \rho)^2(c_{4,0}^2\beta^2 + \frac{169\alpha^2b_{4,0}^2}{30870})\chi^5 + 6174000(c_{4,0}^2\beta^2 + \frac{338\alpha^2b_{4,0}^2}{77175}) \\
& \times(-\delta u_0 + e + \rho)^3\chi^4 - 3087000(c_{4,0}^2\beta^2 + \frac{169\alpha^2b_{4,0}^2}{51450})(-\delta u_0 + e + \rho)^4\chi^3 \\
& + 926100(-\delta u_0 + e + \rho)^5(c_{4,0}^2\beta^2 + \frac{169\alpha^2b_{4,0}^2}{77175})\chi^2 - 154350(c_{4,0}^2\beta^2 + \frac{169\alpha^2b_{4,0}^2}{154350}) \\
& \times(-\delta u_0 + e + \rho)^6\chi - 11025\beta^2\delta^7u_0^7c_{4,0}^2 + 77175c_{4,0}^2\beta^2\delta^6(e + \rho)u_0^6 - 231525c_{4,0}^2\beta^2\delta^5 \\
& \times(e + \rho)^2u_0^5 + 385875c_{4,0}^2\beta^2\delta^4(e + \rho)^3u_0^4 - 385875c_{4,0}^2\beta^2\delta^3(e + \rho)^4u_0^3 + 231525c_{4,0}^2\beta^2\delta^2 \\
& \times(e + \rho)^5u_0^2 - 77175c_{4,0}^2\beta^2\delta(e + \rho)^6u_0 + 11025\beta^2e^7c_{4,0}^2 + 77175\beta^2e^6\rho c_{4,0}^2
\end{aligned}$$

$$\begin{aligned}
& +231525\beta^2 e^5 \rho^2 c_{4,0}^2 + 385875\beta^2 e^4 \rho^3 c_{4,0}^2 + 385875\beta^2 e^3 \rho^4 c_{4,0}^2 + 231525\beta^2 e^2 \rho^5 c_{4,0}^2 \\
& +77175\beta^2 e \rho^6 c_{4,0}^2 + 11025\beta^2 \rho^7 c_{4,0}^2 + 99239431541250\mu^7, \\
a_{2,2} &= -565950 \frac{\mu^4}{\chi (-\delta u_0 - 2\chi + e + \rho)^3}, a_{2,4} = -14700 \frac{\mu^3}{\chi^2 (-\delta u_0 - 2\chi + e + \rho)}, \\
a_{2,6} &= -35420 \frac{\mu^2 (-\delta u_0 - 2\chi + e + \rho)}{\chi^3}, a_{2,8} = 570 \frac{(-\delta u_0 - 2\chi + e + \rho)^3 \mu}{\chi^4}, \\
a_{2,10} &= -6 \frac{(-\delta u_0 - 2\chi + e + \rho)^5}{\chi^5}, a_{4,0} = -\frac{5187875 \mu^4}{3 (-\delta u_0 - 2\chi + e + \rho)^4}, \\
a_{4,2} &= -220500 \frac{\mu^3}{\chi (-\delta u_0 - 2\chi + e + \rho)^2}, a_{4,4} = 37450 \frac{\mu^2}{\chi^2}, \\
a_{4,6} &= -1460 \frac{(-\delta u_0 - 2\chi + e + \rho)^2 \mu}{\chi^3}, a_{4,8} = 15 \frac{(-\delta u_0 - 2\chi + e + \rho)^4}{\chi^4}, \\
a_{6,0} &= \frac{75460 \mu^3}{3 (-\delta u_0 - 2\chi + e + \rho)^3}, a_{6,2} = -18620 \frac{\mu^2}{\chi (-\delta u_0 - 2\chi + e + \rho)}, \\
a_{6,4} &= 1540 \frac{(-\delta u_0 - 2\chi + e + \rho) \mu}{\chi^2}, a_{6,6} = -20 \frac{(-\delta u_0 - 2\chi + e + \rho)^3}{\chi^3}, \\
a_{8,0} &= 735 \frac{\mu^2}{(-\delta u_0 - 2\chi + e + \rho)^2}, a_{8,2} = -690 \frac{\mu}{\chi}, a_{8,4} = 15 \frac{(-\delta u_0 - 2\chi + e + \rho)^2}{\chi^2}, \\
a_{10,0} &= 98 \frac{\mu}{-\delta u_0 - 2\chi + e + \rho}, a_{10,2} = \frac{6\delta u_0 + 12\chi - 6e - 6\rho}{\chi}, b_{0,0} = \frac{539\mu^2 b_{4,0}}{9(-\delta u_0 - 2\chi + e + \rho)^2}, \\
b_{0,2} &= \frac{7\mu b_{4,0}}{3\chi}, b_{0,4} = -\frac{b_{4,0}(-\delta u_0 - 2\chi + e + \rho)^2}{15\chi^2}, b_{0,6} = -\frac{b_{4,0}(-\delta u_0 - 2\chi + e + \rho)^4}{105\mu\chi^3}, \\
b_{2,0} &= 19 \frac{\mu b_{4,0}}{3\delta u_0 + 6\chi - 3e - 3\rho}, b_{2,2} = \frac{38 b_{4,0}(-\delta u_0 - 2\chi + e + \rho)}{21\chi}, \\
b_{2,4} &= -\frac{3 b_{4,0}(-\delta u_0 - 2\chi + e + \rho)^3}{35\mu\chi^2}, b_{4,2} = \frac{b_{4,0}(-\delta u_0 - 2\chi + e + \rho)^2}{21\mu\chi}, \\
b_{6,0} &= \frac{b_{4,0}(-\delta u_0 - 2\chi + e + \rho)}{21\mu}, c_{0,0} = \frac{12005\mu^2 c_{4,0}}{39(-\delta u_0 - 2\chi + e + \rho)^2}, c_{0,2} = -\frac{535\mu c_{4,0}}{13\chi}, \\
c_{0,4} &= \frac{45 c_{4,0}(-\delta u_0 - 2\chi + e + \rho)^2}{13\chi^2}, c_{0,6} = -\frac{5 c_{4,0}(-\delta u_0 - 2\chi + e + \rho)^4}{13\mu\chi^3}, \\
c_{2,0} &= 245 \frac{\mu c_{4,0}}{13\delta u_0 + 26\chi - 13e - 13\rho}, c_{2,2} = \frac{230 c_{4,0}(-\delta u_0 - 2\chi + e + \rho)}{13\chi}, \\
c_{2,4} &= -\frac{5 c_{4,0}(-\delta u_0 - 2\chi + e + \rho)^3}{13\mu\chi^2}, c_{4,2} = \frac{9 c_{4,0}(-\delta u_0 - 2\chi + e + \rho)^2}{13\mu\chi}, \\
c_{6,0} &= \frac{c_{4,0}(-\delta u_0 - 2\chi + e + \rho)}{13\mu}, \tag{4.11}
\end{aligned}$$

where $b_{4,0}$ and $c_{4,0}$ are arbitrary constants.

In Figures 11 and 12, the three high peaks of the third-order rogue waves for (4.6) at $\alpha = \beta = 0$ are introduced. The third-order peak breaks apart and for sufficiently big parameters for $\alpha = \beta = 10^8$, the

third-order rogue waves consists of five first-order rogue waves are located in the corners of a pentagon and other one sites in the center.

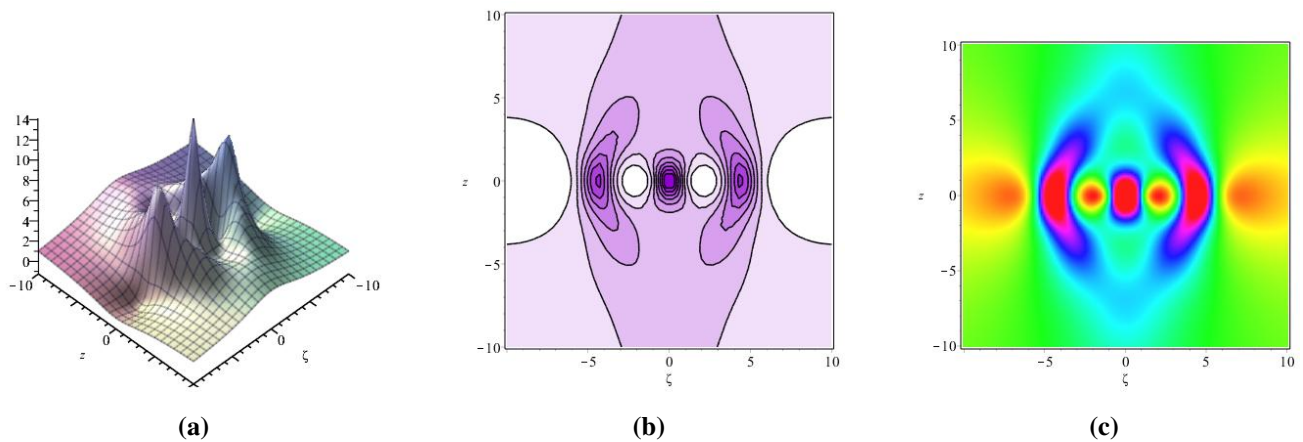


Figure 11. The third-order rogue wave solution (4.10). (a) 3D plot; (b) Contour plot; (c) Density at $\alpha = \beta = 0$.

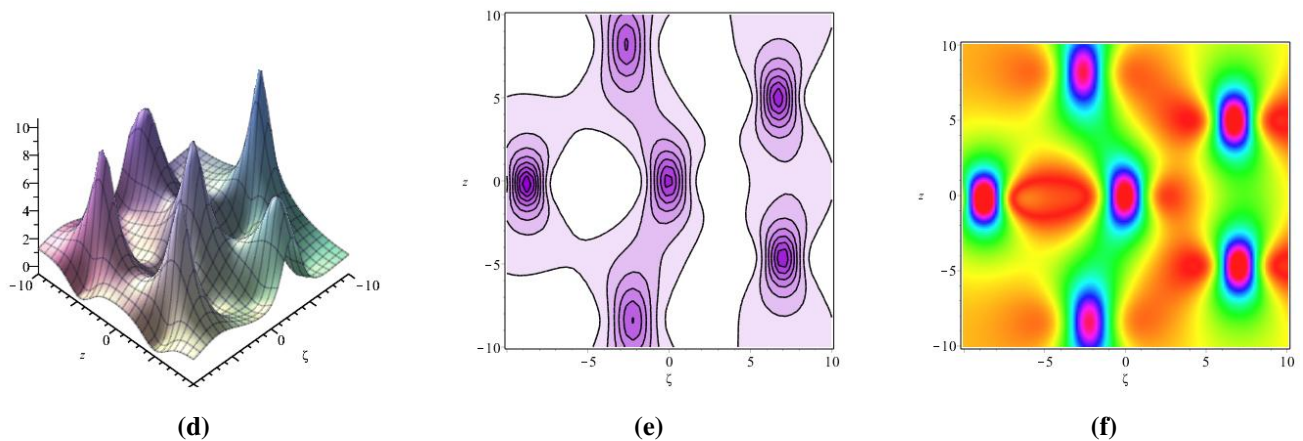


Figure 12. The third-order rogue wave solution (4.10). (a) 3D plot; (b) Contour plot; (c) Density at $\alpha = \beta = 10^8$.

5. Conclusions

In this paper, we investigated the first, second, and third-order rogue waves for two (3+1)-dimensional extensions of the (KP) equation by the bilinear method via the symbolic computation approach. The properties of the two (3+1)-dimensional extensions of the (KP) equation are examined by introducing several figures. The obtained higher-order rogue waves have the property $\lim_{x \rightarrow \pm\infty} = \lim_{y \rightarrow \pm\infty} = \lim_{z \rightarrow \pm\infty} = \lim_{t \rightarrow \pm\infty} = u_0$. The figures were depicted in three dimensional, contour and density with the center controlled by the parameters α and β . The results obtained in this work are useful to understand the dynamic behaviors of higher-rogue waves in the deep ocean and nonlinear optical fibers. Thus, the characteristics of these solutions are discussed through some diverting graphics under different parameter choices. The dynamics behaviors of higher-rogue waves related to the optical rogue waves are pulses of light similar to rogue or freak ocean waves. Rogue waves in optical fibers can be described mathematically by the nonlinear

Schrödinger equation and its extensions that take into account third-order dispersion. We can apply this technique to completely integrable nonlinear evolution equations.

Acknowledgments

The authors extend their appreciation to the Deanship of Scientific Research at King Khalid University, Abha, Saudi Arabia, for funding this work through the Research Group Project under Grant Number (RGP. 2/36/43). This research was funded by Princess Nourah bint Abdulrahman University Researchers Supporting Project number (PNURSP2022R229), Princess Nourah bint Abdulrahman University, Riyadh, Saudi Arabia.

Conflict of interest

All authors declare that they have no conflicts of interest.

References

1. W. R. Sun, B. Tian, H. L. Zhen, Y. Sun, Breathers and rogue waves of the fifth-order nonlinear Schrödinger equation in the Heisenberg ferromagnetic spin chain, *Nonlinear Dyn.*, **81** (2015), 725–732. <https://doi.org/10.1007/s11071-015-2022-4>
2. X. Y. Xie, B. Tian, Y. F. Wang, Y. Sun, Y. Jiang, Rogue wave solutions for a generalized nonautonomous nonlinear equation in a nonlinear inhomogeneous fiber, *Ann. Phys.*, **362** (2015), 884–892. <https://doi.org/10.1016/j.aop.2015.09.001>
3. C. Kharif, E. Pelinovsky, A. Slunyaev, *Rogue waves in the ocean: Observations, theories and modeling*, Advances in Geophysical and Environmental Mechanics and Mathematics Series, Springer, Berlin, 2009.
4. A. Osborne, *Nonlinear ocean waves and the inverse scattering transform*, Elsevier, New York, 2010.
5. N. Akhmediev, A. Ankiewicz, M. Taki, Waves that appear from nowhere and disappear without a trace, *Phys. Lett. A*, **373** (2009), 675–678. <https://doi.org/10.1016/j.physleta.2008.12.036>
6. N. Akhmediev, J. M. Soto-Crespo, A. Ankiewicz, Extreme waves that appear from nowhere: on the nature of rogue waves, *Phys. Lett. A*, **373** (2009), 2137–2145. <https://doi.org/10.1016/j.physleta.2009.04.023>
7. E. Pelinovsky, C. Kharif, *Extreme ocean waves*, Springer, Berlin 2008. <https://doi.org/10.1007/978-1-4020-8314-3>
8. P. A. Clarkson, E. Dowie, Rational solutions of the Boussinesq equation and applications to rogue waves, *Trans. Math. Appl.*, **1** (2017), 1–26. <https://doi.org/10.1093/imatrm/tnx003>
9. A. N. Ganshin, V. B. Efimov, G. V. Kolmakov, L. P. Mezhov-Deglin, P. V. E. McClintock, Observation of an inverse energy cascade in developed acoustic turbulence in superfluid helium, *Phys. Rev. Lett.*, **101** (2008), 065303. <https://doi.org/10.1103/PhysRevLett.101.065303>

10. B. Kibler, J. Fatome, C. Finot, G. Millot, F. Dias, G. Genty, et al., The Peregrine soliton in nonlinear fibre optics, *Nature Phys.*, **6** (2010), 790–795. <https://doi.org/10.1038/nphys1740>
11. J. He, L. Guo, Y. Zhang, A. Chabchoub, Theoretical and experimental evidence of non-symmetric doubly localized rogue waves, *Proc. Math. Phys. Eng. Sci.*, **470** (2014), 20140318. <https://doi.org/10.1098/rspa.2014.0318>
12. A. Chabchoub, N. P. Hoffmann, N. Akhmediev, Rogue wave observation in a water wave tank, *Phys. Rev. Lett.*, **106** (2011), 204502. <https://doi.org/10.1103/PhysRevLett.106.204502>
13. F. Demontis, B. Prinari, C. van der Mee, F. Vitale, The inverse scattering transform for the focusing nonlinear Schrodinger equation with asymmetric boundary conditions, *J. Math. Phys.*, **55** (2014), 101505. <https://doi.org/10.1063/1.4898768>
14. W. Liu, Y. Zhang, Families of exact solutions of the generalized (3+1)-dimensional nonlinear-wave equation, *Mod. Phys. Lett. B*, **32** (2018), 1850359. <https://doi.org/10.1142/S0217984918503591>
15. B. Guo, L. Ling, Q. P. Liu, Nonlinear Schrödinger equation: Generalized Darboux transformation and rogue wave solutions, *Phys. Rev. E*, **85** (2012), 026607. <https://doi.org/10.1103/PhysRevE.85.026607>
16. X. W. Yan, S. F. Tian, M. J. Dong, L. Zou, Bäcklund transformation, rogue wave solutions and interaction phenomena for a (3+1)-dimensional B-type Kadomtsev-Petviashvili-Boussinesq equation, *Nonlinear Dyn.*, **92** (2018), 709–720. <https://doi.org/10.1007/s11071-018-4085-5>
17. K. J. Wang, Periodic solution of the time-space fractional complex nonlinear Fokas-Lenells equation by an ancient Chinese algorithm, *Optik*, **243** (2021), 167461. <https://doi.org/10.1016/j.ijleo.2021.167461>
18. K. J. Wang, G. D. Wang, Variational theory and new abundant solutions to the (1+2)-dimensional chiral nonlinear Schrödinger equation in optics, *Phys. Lett. A*, **412** (2021), 127588. <https://doi.org/10.1016/j.physleta.2021.127588>
19. K. J. Wang, G. D. Wang, Study on the explicit solutions of the Benney-Luke equation via the variational direct method, *Math. Methods Appl. Sci.*, **44** (2021), 14173–14183. <https://doi.org/10.1002/mma.7683>
20. B. B. Kadomtsev, V. I. Petviashvili, On the stability of solitary waves in weakly dispersive media, *Sov. Phys. Dokl.*, **15** (1970), 539–541.
21. M. K. Elboree, Higher order rogue waves for the (3+1)-dimensional Jimbo-Miwa equation, *Int. J. Nonlinear Sci. Numer. Simul.*, 2021. <https://doi.org/10.1515/ijnsns-2020-0065>
22. W. Liu, Y. Zhang, Multiple rogue wave solutions for a (3+1)-dimensional Hirota bilinear equation, *Appl. Math. Lett.*, **98** (2019), 184–190. <https://doi.org/10.1016/j.aml.2019.05.047>
23. M. S. Ullah, H. O. Roshid, F. S. Alshammari, M. Z. Ali, Collision phenomena among the solitons, periodic and Jacobi elliptic functions to a (3+1)-dimensional Sharma-Tasso-Olver-like model, *Results Phys.*, **36** (2022), 105412. <https://doi.org/10.1016/j.rinp.2022.105412>
24. H. O. Roshid, N. F. M. Noor, M. S. Khatun, H. M. Baskonus, F. B. M. Belgacem, Breather, multi-shock waves and localized excitation structure solutions to the extended BKP-Boussinesq equation, *Commun. Nonlinear Sci. Numer. Simul.*, **101** (2021), 105867. <https://doi.org/10.1016/j.cnsns.2021.105867>

25. R. Li, X. Geng, Rogue periodic waves of the sine-Gordon equation, *Appl. Math. Lett.*, **102** (2020), 106147. <https://doi.org/10.1016/j.aml.2019.106147>
26. M. Zheng, X. Dong, C. Chen, M. Li, Multiple-order rogue wave solutions to a (2+1)-dimensional Boussinesq type equation, *Commun. Theor. Phys.*, **74** (2022), 085002.
27. J. G. Liu, W. H. Zhu, Multiple rogue wave solutions for (2+1)-dimensional Boussinesq equation, *Chin. J. Phys.*, **67** (2020), 492–500. <https://doi.org/10.1016/j.cjph.2020.08.008>
28. J. G. Rao, Y. B. Liu, C. Qian, J. S. He, Rogue waves and Hybrid solutions of the Boussinesq equation, *Z. Naturforsch. A*, **72** (2017), 307–314.
29. Z. Zhao, L. He, Multiple lump solutions of the (3+1)-dimensional potential Yu-Toda-Sasa-Fukuyama equation, *Appl. Math. Lett.*, **95** (2019), 114–121. <https://doi.org/10.1016/j.aml.2019.03.031>
30. Z. Zhao, L. He, Resonance Y-type soliton and hybrid solutions of a (2+1)-dimensional asymmetrical Nizhnik-Novikov-Veselov equation, *Appl. Math. Lett.*, **122** (2021), 107497. <https://doi.org/10.1016/j.aml.2021.107497>
31. L. He, Z. Zhao, Multiple lump solutions and dynamics of the generalized (3+1)-dimensional KP equation, *Mod. Phys. Lett. B*, **34** (2020), 2050167. <https://doi.org/10.1142/S0217984920501675>
32. Zhaqilao, A symbolic computation approach to constructing rogue waves with a controllable center in the nonlinear systems, *Comput. Math. Appl.*, **75** (2018), 3331–3342. <https://doi.org/10.1016/j.camwa.2018.02.001>
33. R. Hirota, Direct method in soliton theory, In: R. K. Bullough, P. J. Caudrey, *Solitons*, Springer, Berlin, 1980. https://doi.org/10.1007/978-3-642-81448-8_5
34. A. M. Wazwaz, Multiple soliton solutions for two (3+1)-dimensional extensions of the KP equation, *Int. J. Nonlinear Sci.*, **12** (2011), 471–477.



AIMS Press

©2022 the Author(s), licensee AIMS Press. This is an open access article distributed under the terms of the Creative Commons Attribution License (<http://creativecommons.org/licenses/by/4.0>)